IEEE Open Journal of
Power Electronics

Received 5 June 2020; revised 9 July 2020; accepted 15 July 2020. Date of publication 22 July 2020;
date of current version 6 August 2020.

*Digital Object Identifier 10.1109/OJPEL.2020.3011174*

# A T-Type DC-DC Converter With Reduced Middle-Leg Switch Current Stress and Improved Light-Load Efficiency

**JAVAD KHODABAKHSH [1] (Student Member, IEEE), AND GERRY MOSCHOPOULOS [2] (Senior Member, IEEE)**

[1] Department of Electrical and Computer Engineering, Western University Faculty of Engineering, London N6A 3K7, U.K.
[2] Department of Electrical and Computer Engineering, Western University, Canada, London N6A5B9, U.K.

CORRESPONDING AUTHOR: JAVAD KHODABAKHSH (e-mail: jkhodaba@uwo.ca)

This work was supported by the Natural Sciences and Engineering Research Council (NSERC) of Canada.

**ABSTRACT** The ZVS T-type converter can be used as an alternative to the conventional ZVS-PWM full-bridge (FB) converter for applications where improved light-load operation is required. In this converter, two of the switches conduct only the current that flows during a freewheeling mode of operation and two of the switches conduct only the current that flows in the converter when it is in an energy-transfer mode. This is unlike the switches in the ZVS-PWM-FB converter that must conduct both currents. Although the ZVS T-type converter needs less inductive energy to achieve ZVS in its switches, it has a higher primary current during its freewheeling modes than the ZVS-PWM-FB converter because it is basically a half-bridge converter. In this paper, the use of ZVZCS methods to reduce the RMS value of the current in switches that are used in the freewheeling current path is investigated. The operation of the ZVS-PWM T-type converter and a T-type converter operating with ZVZCS are reviewed and compared analytically. Experimental results obtained from prototypes of the two converters along with results from prototypes of the standard ZVS-PWM-FB converter and a ZVZCS-PWM-FB converter are presented. It is demonstrated that a T-type converter with ZVZCS has a better light-load efficiency than the ZVS-PWM-FB and the ZVS T-type converters and that the current stress in its middle-leg switches is much smaller; thus, it can be implemented with much smaller and inexpensive middle-leg switches.

**INDEX TERMS** DC-DC power conversion, Zero voltage switching (ZVS), Zero-voltage-zero-current switching (ZVZCS), ZVS T-Type converter.

## I. INTRODUCTION

The conventional zero-voltage (ZVS), pulse width modulated (PWM) full-bridge (FB) DC-DC converter is a popular converter that is widely used in many industrial applications [1]–[3] because its switches can operate with ZVS under heavy-load conditions without the need for additional auxiliary circuitry. The converter, however, has several drawbacks, including the following:

- The converter switches lose their ZVS operating capability when the converter operates with light loads, as there is not enough leakage inductance energy to discharge the output capacitances of the switches before they are turned on. There is, however, a trade-off between ZVS operation range and leakage inductance that must be considered as adding more leakage inductance increases the load range for ZVS, but at the cost of increasing duty cycle loss and power losses, especially for heavy-load operation [4]–[7].
- When the converter is in a freewheeling mode of operation, current circulates through two converter devices and creates conduction losses without any energy transfer happening. The converter switches also have more RMS current stresses [8]–[10].
- It is challenging to prevent saturation in the converter's transformer. Sophisticated sensing methods to monitor and adjust the volt-seconds applied to a transformer [11]–[13] or a DC blocking capacitor in series with the transformer [15], [16] are needed, but each method is disadvantageous in some way.

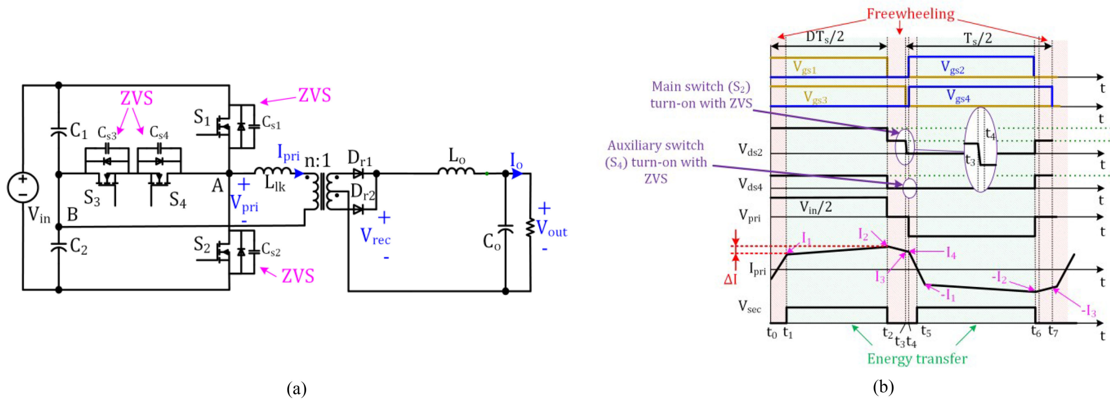


**FIG. 1.** The ZVS T-type DC-DC converter (a) Converter schematic, (b) Typical waveforms.

An alternative to the conventional ZVS-PWM-FB DC-DC converter that does not have these drawbacks is the ZVS T-type converter (Fig. 1(a)) that proposed in [16]. The performance of this converter was compared by the authors of this paper to that of the ZVS-PWM-FB converter in [17]. It was demonstrated in [17] that, unlike ZVS-PWM-FB converters, the voltage across the switches in ZVS T-type converters is half of the input voltage before they are switched on; thus, when the converter operates under light load conditions and switches lose their ZVS capability, a T-Type converter has lower switching losses than a ZVS-PWM-FB. In many applications, light-load efficiency is important as the converter operates under light-load conditions for most of the time and under heavy-load conditions occasionally.

Regulatory programs such as Energy Star [18], which is run by the U.S. Environmental Protection Agency (EPA) and the U.S. Department of Energy (DOE) to promote energy efficiency, now demand strict compliance with light-load efficiency specifications. According to [18] the light-load efficiency of an AC-DC power supply unit (PSU) with 1 kW rating for server applications should be higher than 80% if it is operating in the range of 20% - 50% of full-load. For a two-stage AC-DC converter, this means that the back-end DC-DC converter must have a high light-load efficiency as the overall efficiency of the two-stage converter is the product of the efficiency of the AC-DC front-end converter and that of the DC-DC back-end converter. As a result, the need for light-load efficiency improvement has spurred research in DC-DC converters in recent years. Such improvement can be achieved through new topologies, like the one proposed in [19], which improves the light-load efficiency in FB converters by almost 3%, or through new control strategies, like the one proposed in [20], which improved light-load efficiency by 2.5%.

The main drawback of the ZVS T-type converter, however, is the fact that it has twice as much current flowing through its primary side than does the ZVS-PWM-FB converter so that it has more current circulating in its primary whenever it is in a freewheeling mode of operation (i.e., no voltage impressed across its primary). The main focus of this paper is to investigate the operation of T-type converter with ZVZCS methods that have been shown to reduce freewheeling. circulating current in PWM full-bridge converters [21]–[24] This paper examines the effectiveness of ZVZCS in order to

- reduce conduction losses in the T-type converter as a way to improve light-load efficiency, given that conduction losses caused by freewheeling mode current are the main drawback in this converter;
- reduce RMS current stress in middle leg switches ($S_3$ and $S_4$) as these switches conduct only freewheeling current.

It should be noted that the novelty of this paper is not so much with the way ZVZCS is implemented in a T-type converter as many ZVZCS methods have been proposed for the standard full-bridge converter in the literature and a commonly-used method has been selected for this paper. The main contribution of this paper is the use of ZVZCS as a way to improve light-load efficiency and reduce current stresses in the middle-leg switches in a T-type converter, to improve upon the work that the authors presented in [25]. The addition of ZVZCS to a T-type converter results in characteristics that have not been reported in the literature.

In this paper, the basic operating principles of the ZVS T-type converter and a modified ZVZCS T-type converter are explained in Section II. In Section III, the ZVZCS converter's features are explained. In Section IV, a design procedure for the the ZVZCS converter is presented. In Section V, the most significant power losses of the two converters are compared. In Section VI, experimental results obtained from prototypes of the two converters as well as results obtained from prototypes of a ZVS-PWM FB converter and a ZVZCS-PWM-FB are presented and compared. The paper ends with a brief summary of the main points of the paper and with conclusions in Section VII.

## II. OPERATION PRINCIPLES OF ZVS T-TYPE CONVERTER AND ZVZCS T-TYPE CONVERTER

The basic operation of the ZVS T-type converter and the modified ZVZCS T-type converter is explained in this section of the paper.

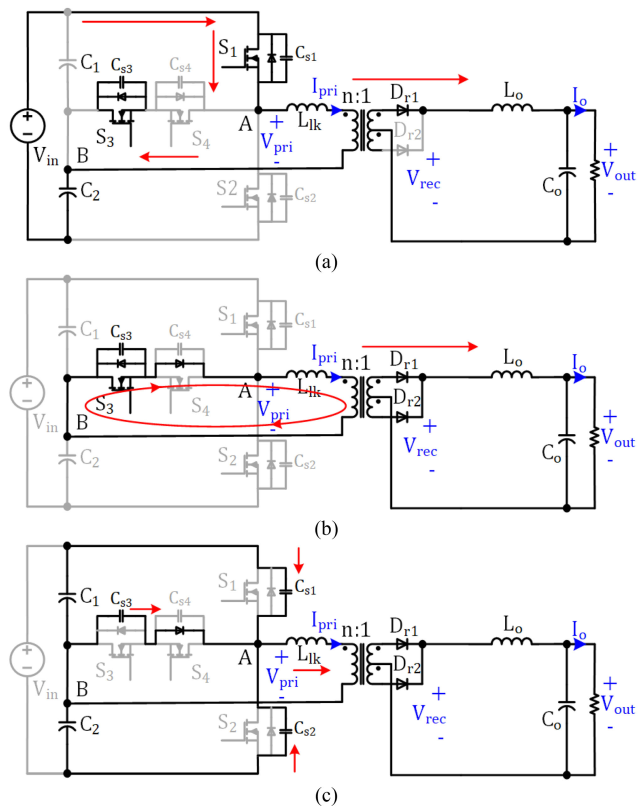


**FIG. 2.** **Typical modes of operation (a) energy transfer mode, (b) freewheeling mode (c) transition from freewheeling to energy transition mode.**

### A. ZVS T-TYPE CONVERTER

The DC-DC ZVS T-type converter shown in Fig. 1(a) consists of two main switches ($S_1$ and $S_2$), two auxiliary switches ($S_3$ and $S_4$), a split-capacitor DC bus ($C_1$–$C_2$), a transformer with turns ratio equal to n:1 and leakage inductance ($L_{lk}$), two secondary rectifying diodes ($D_{r1}$-$D_{r2}$), and an LC filter consisting of output inductor ($L_o$) and output capacitor ($C_o$). The converter has energy transfer, freewheeling, and transition modes of operation. The modes of operation of the ZVS T-type converter for half of a switching cycle are described as follows, with an equivalent circuit diagram for each mode shown in Fig. 2:

#### 1) ENERGY TRANSFER MODE($T_1<T<T_2$)

A typical energy transfer mode is shown in Fig. 2(a). During this mode, either $S_1$ or $S_2$ is on and point "A" is connected to $V_{in}$ or zero, respectively. For each case, half of the input voltage is applied to the transformer primary winding ($V_{pri}$) as point "B" is connected to a fixed voltage ($V_{in}/2$). In this mode, one of the two rectifying diodes conducts and $V_{rec}$ is equal to $V_{in}/2n$; energy can be transferred from the primary side to the output filter and load. The primary current during this mode can be expressed as

$$I_{pri}(t) = I_1 + \frac{\left(\frac{V_{in}}{2} - nV_o\right)}{L_o} t \tag{1}$$

#### 2) FREEWHEELING MODE($T_2<T<T_3$)

A typical freewheeling mode is shown in Fig. 2(b). During this mode, one of the middle leg switches ($S_3$ or $S_4$) is on. Point "A" and point "B" are connected and $V_{pri}$ is equal to zero. In this mode, $V_{rec}$ is equal to zero and power does not transfer from the primary to the secondary. Current circulates through the transformer primary windings, a middle-leg switch, and the body diode of the other middle-leg switch. The primary current during this mode can be expressed as

$$I_{pri}(t) = I_2 e^{-\left(\frac{R_{ds-LV}}{L_{lk}}\right)t} = I_2 e^{-\frac{t}{\tau}} \tag{2}$$

where $R_{ds-LV}$ denotes the on-state resistance one of the auxiliary switches It should be noted that $1/\tau \gg t_3 - t_2$ so that (2) can be estimated to be

$$I_{pri}(t) = I_2\left(1 - \frac{t}{\tau}\right) \tag{3}$$

#### 3) TRANSITION MODE($T_3<T<T_4$)

When the freewheeling mode ends, a dead time equal to $D_{dead}T_s$ is inserted before the next energy-transfer mode to discharge the parasitic capacitor of the main switch; this mode is shown in Fig. 2(c). In this mode, sufficient energy should be available in the transformer's primary leakage inductance to discharge/charge the parasitic capacitors, which have a voltage of $V_{in}/2$ across them. At the end of this mode, the next set of main and middle leg switches can be turned on with ZVS as shown in Fig. 1(b). The primary current at the end of this mode can be expressed as

$$|I_4| = |I_3| \cos\omega_0 (D_{dead}T_s) \tag{4}$$

where $\omega_0$ is defined as

$$\omega_0 = \frac{1}{\sqrt{L_{lk}(2C_{S-HV} + C_{S-LV})}} \tag{5}$$

where $C_{S-HV}$ and $C_{S-LV}$ denote the parasitic capacitances of the main and middle-leg switches respectively. The converter switches are operating with ZVS if $I_3$ and $I_4$ have the same sign. More details about the operation of the ZVS T-Type converter operation can be found in [17].

### B. ZVZCS T-TYPE CONVERTER

The modified T-type converter (ZVZCS T-type converter), shown in Fig. 3(a) has the same components as the ZVS T-Type converter, but with the simple auxiliary circuit proposed in [26] added to extinguish the circulating current in the freewheeling mode. The auxiliary circuit consists of three diodes ($D_f$, $D_1$, and $D_2$) and a capacitor, $C_{aux}$. It should be noted that various methods have been proposed to extinguish the circulating current in various ZVZCS-PWM topologies and that this particular auxiliary circuit has selected because of its simplicity; more sophisticated auxiliary circuits can be used if desired.

The ZVZCS T-type converter has the same operation modes as the ZVS T-type converter: energy transfer, freewheeling, and transition modes. The modes of operation of the ZVZCS T-type converter for a switching cycle are explained below,

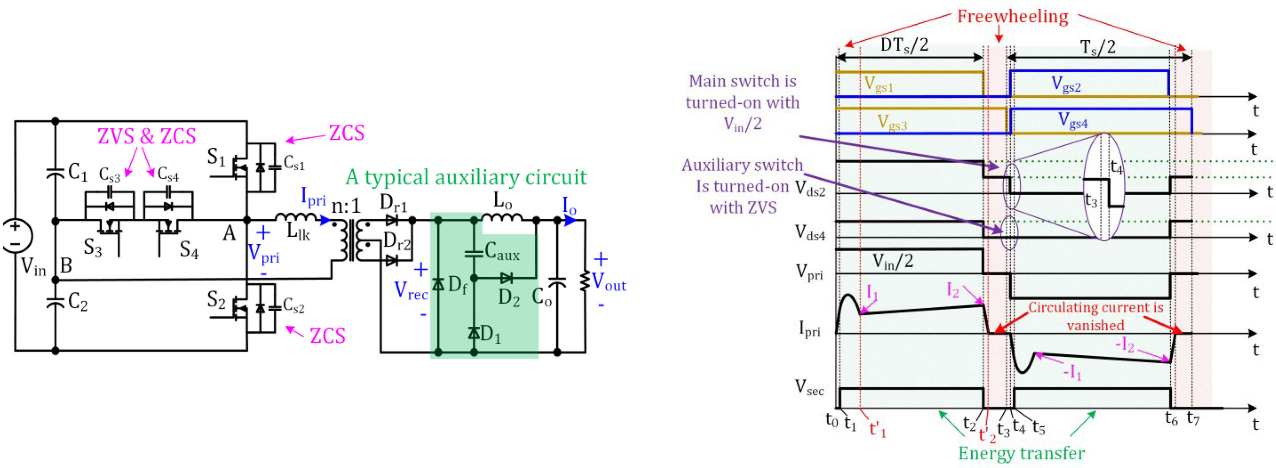


(a) (b)

**FIG. 3.** The ZVZCS T-type DC-DC converter (a) Converter schematic, (b) Typical waveforms.

with an equivalent circuit diagram for each mode shown in Fig. 4. It should be noted that these modes are valid for both heavy-load and light-load operating conditions except that the output inductor current may fall to zero during a freewheeling mode when the converter is operating with light loads.

#### 1) ENERGY TRANSFER MODE ($T_1<T<T'_2$)

An energy-transfer mode in the ZVZCS T-Type converter begins when one of the main switches is turned on. This mode can be divided into three sub-modes:

In Sub-Mode 1 ($t_1 < t < t_1'$), $C_{aux}$ resonates with $L_{lk}$ for half the cycle. The equivalent circuit diagram of this sub-mode is shown in Fig. 4(a). The primary current during Sub-Mode 1 can be expressed as

$$I_{pri}(t) = \frac{I_{Lo}}{n} + \frac{V_{in}/2 - nV_o}{Z_1} sin\omega_1 t = \frac{I_{Lo}}{n} + I_{peak} sin\omega_1 t \quad (6)$$

where $Z_1$ and $\omega_1$ are the characteristic impedance and resonant frequency of the resonant tank and are defined as

$$Z_1 = \sqrt{\frac{L_{lk}}{C_{aux}/n^2}} \quad (7)$$

$$\omega_1 = \frac{1}{\sqrt{L_{lk} C_{aux}/n^2}} \quad (8)$$

This mode ends when the voltage across $C_{aux}$ reaches to

$$V_{Caux}\left(t_1'\right) = \frac{V_{in}}{n} - 2.V_o \quad (9)$$

In Sub-Mode 2 ($t_1' < t < t_2$), shown in Fig. 4(b), the converter operation is the same as the ZVS T-Type converter and the primary current equation is the same as that of the ZVS T-type converter during an energy-transfer mode, as defined in (1).

In Sub-Mode 3 ($t_2 < t < t'_2$), shown in Fig. 4(c), the main switches are turned off and one of the auxiliary switches is on. The voltage of $C_{aux}$ is reflected to the transformer primary and is a negative voltage with reverse polarity that is applied to the leakage inductance to extinguish the current that is circulating in the primary. As shown in Fig. 3(b), a finite time is required to extinguish this circulating current; this time can be estimated to be

$$\Delta t = \frac{I_2 L_{lk}}{n V_{Caux}(t_2)} \quad (10)$$

#### 2) ZERO MODE ($T_2<T<T_3$)

In this mode shown in Fig. 4(d), the primary current is zero; thus, the voltage across the main switches is half of the input voltage. Since no current flows through $C_{aux}$ in this zero mode ($t_2' < t < t_3$) of the energy transfer mode, the voltage across the $C_{aux}$ remains constant in this mode.

#### 3) TRANSITION MODE ($T_3<T<T_4$)

During a transition mode (Fig. 4(e)), the primary current is zero and energy is transferred from the output inductor ($L_o$) and capacitor ($C_o$) to the load. At the end of this mode, one of the main switches is turned on with a reduced voltage ($V_{in}/2$) so that turn-on losses can be reduced significantly, and a middle-leg switch is turned on with ZVS, as the voltage at each end of the switch is the same $V_{in}/2$.

#### 4) FREEWHEELING MODE ($T_4<T<T_5$):

At the start of this mode, the other main switch ($S_2$) and auxiliary switch ($S_4$) are turned on as shown in Fig. 4(f). Half of the input voltage with negative polarity ($-V_{in}/2$) is applied to the primary winding and the absolute value of the primary current increases with the rate of $V_{in}/2L_{lk}$. While the primary current is less than $I_1/n$, the $V_{rec}$ at the secondary is zero and the inductor current circulates through $D_f$, $D_{r1}$ and $D_{r2}$. This mode ends when the primary current reaches $I_1/n$.

## III. ZVZCS T-TYPE CONVERTER FEATURES

The ZVZCS T-type converter has the following features:

- The maximum voltage that is applied to the main switches of the converter ($S_1$ and $S_2$) is equal to the input

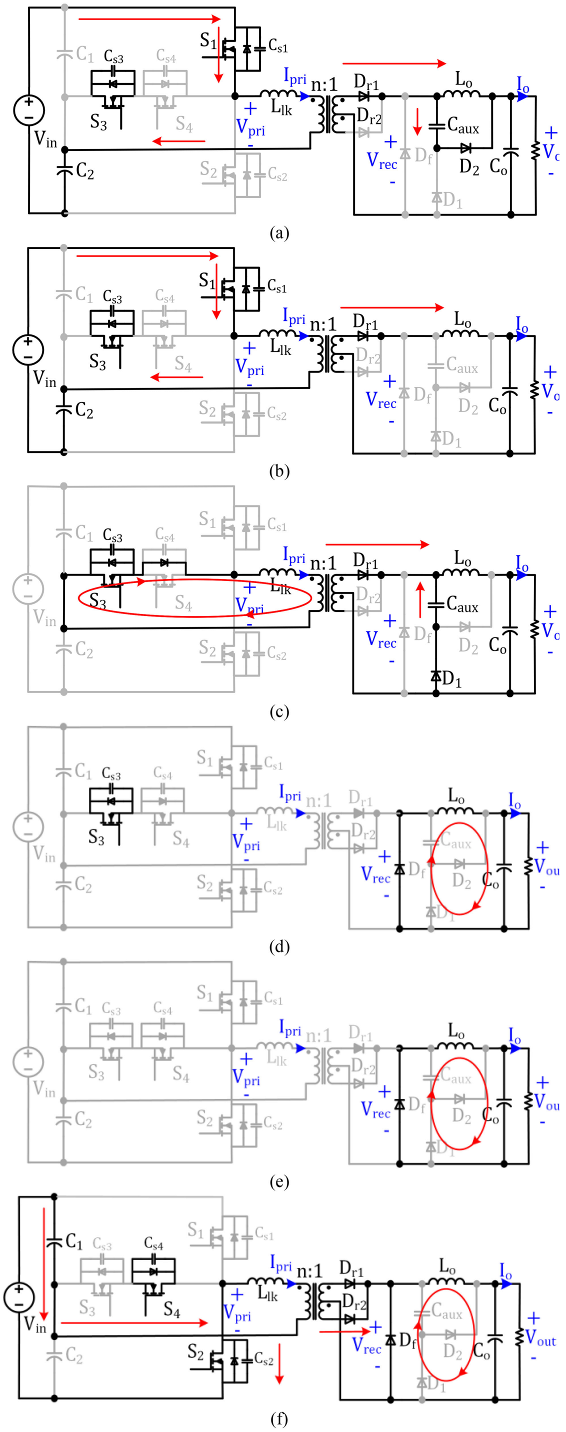


**FIG. 4.** **Typical modes of operation (a) energy transfer mode sub-mode 1 (t), (b) energy transfer mode sub-mode 2, (c) energy transfer mode sub-mode 3 (d) zero mode, (e) transition mode, (f) freewheeling mode.**

voltage, but the voltage falls to $V_{in}/2$ before turn-on. When the converter enters into a freewheeling mode, the main switches are turned off and the voltage at the mid-point of the main leg is $V_{in}/2$ because of the voltage division between the parasitic capacitors of the main switches. The auxiliary circuit extinguishes the current circulating in the primary side so that that the voltage at the mid-point of the main leg remains at $V_{in}/2$. It should be noted that the middle leg switches of both T-type converters block $V_{in}/2$ voltage.

- The middle-leg switches must block a maximum voltage that is just half of the input voltage. Moreover, the current that flows in the middle-leg switches is very small as each of these switches conducts just the freewheeling current for only half the time that the converter is in a freewheeling mode of operation. Since the freewheeling current is extinguished by the secondary auxiliary circuit, the power losses in the middle-leg switches are negligible. This allows cheaper, smaller, lower-rated devices with higher values of on-state resistance to be used in the converter.

## IV. ZVZCS T-TYPE CONVERTER DESIGN

A design procedure for the key parameters of the ZVZCS T-type converter is shown in this section and then demonstrated with a design example. For the design example, the ZVZCS T-type converter is designed according to the following specifications: Input voltage $V_{in} = 400$ V, output voltage $V_o = 48$ V, maximum output power $P_{o,max} = 900$ W, minimum output power $P_{o,min} = 45$ W, and switching frequency $f_{sw} = 50$ kHz. The converter delivers the nominal voltage with $D = 0.6$, where $D$ is related to the time span from $t_1$ to $t_2$. The transformer turns ratio (n) is selected in the same manner as in [17]. The voltage divider capacitors and output filter are designed in the same manner as in [17] and [27], respectively. The auxiliary circuit components are designed with the same method as in [24].

### A. MAIN SWITCHES ($S_1$ AND $S_2$)

It can be seen from Fig. 3(b) that the main switches of the converter must block the DC bus voltage ($V_{in}$) when they are off. The current ratings of the main switches can be determined based on the current they conduct during energy-transfer and freewheeling modes of operation to simplify the comparison between the ZVZCS and ZVS T-type converter. To do so, the converter primary current can be into two components: energy- transfer and freewheeling current; these are designated below by the subscripts 'et' and 'fw', respectively.

The rms and average values of the current in the switches during energy-transfer modes can be expressed as follows:

$$I_{et-ave-T} = \frac{1}{\frac{T_s}{2}}\left(\begin{array}{l}\int_0^{D\frac{T_s}{2}}\left(I_1 + \frac{(I_2-I_1)}{DT_s}t\right)dt \\ + \int_0^{\frac{\pi}{\omega_1}} I_{peak}\sin\omega_1 t\,dt\end{array}\right) = \left(\frac{I_1+I_2}{2}\right)D + \frac{2}{T_s\omega_1}I_{peak} \qquad (11)$$

$$I_{et-rms-T} = \sqrt{\frac{1}{\frac{T_s}{2}}\left(\begin{array}{l}\int_0^{D\frac{T_s}{2}}\left(I_1 + \frac{(I_2-I_1)}{DT_s}t\right)^2 dt \\ + \int_0^{\frac{\pi}{\omega_1}}\left(I_{peak}\sin\omega_1 t\right)^2 dt\end{array}\right)}$$

$$\times\sqrt{D\left(I_2 I_1+\frac{1}{3}(I_2-I_1)^2\right)+\frac{\pi}{T_s\omega_1}I_{peak}^2} \tag{12}$$

$$I_{fw-ave}=\frac{1}{\frac{T_s}{2}}\int_0^{\Delta t} I_{pri}(t)\,dt$$
$$=\frac{2}{T_s}\int_0^{\Delta t}\left(I_2-\left(\frac{I_2}{\Delta t}\right)t\right)dt=I_2\frac{\Delta t}{2T_s} \tag{13}$$

$$I_{fw-rms}=\sqrt{\frac{1}{\frac{T_s}{2}}\int_0^{\Delta t} I_{pri}^2(t)\,dt}=\sqrt{\frac{2}{T_s}\int_0^{\Delta t}\left(I_2-\left(\frac{I_2}{\Delta t}\right)t\right)^2 dt}$$
$$=I_2\sqrt{\frac{2\Delta t}{3T_s}} \tag{14}$$

In (11) and (12), the second terms show the effect of ZVZCS on the primary current values during energy-transfer modes, which are independent of the converter load.

The current ratings of the main switches can be calculated based on (11) and (12). Based on the fact that each main switch carries energy-transfer current in each half switching period, the current ratings for the main switches can be determined to be

$$I_{SHV-ave}=\frac{I_{et-ave}}{2} \tag{15}$$

$$I_{SHV-rms}=\frac{I_{et-rms}}{\sqrt{2}} \tag{16}$$

The rated values for the main switches in this design example are

$$I_{\mathrm{SHV}-ave}=2.3A$$
$$I_{\mathrm{SHV}-rms}=4A$$

### B. MIDDLE-LEG SWITCHES ($S_3$ AND $S_4$)

It can be seen from Fig. 3(b) that the maximum voltage that is applied to the auxiliary switches of the ZVZCS T-type converter is half of the DC bus voltage ($V_{in}/2$). The middle-leg switches carry the transformer primary current when the converter exits from an energy-transfer mode, however, the freewheeling current is quickly extinguished. Current flows through a middle-leg switch and the body-diode of the other middle-leg switch during each freewheeling mode. The average current of each switch can be expressed as

$$I_{SLV-ave}=\frac{I_{fw-ave}}{2} \tag{17}$$

and the RMS current for the middle-leg switches can be expressed as

$$I_{SLV-rms}=\frac{I_{fw-rms}}{\sqrt{2}} \tag{18}$$

In this design example, the rated value of current of the auxiliary switches are

$$I_{\mathrm{SLV}-ave-T}=0.01A$$
$$I_{\mathrm{SLV}-rms-T}=0.35A$$

The middle-leg switch average and rms currents for a ZVS T-type converter with the same specifications converter are 3A and 4.5A, respectively. It can be seen that two small switches with a very low current rating can be used as the middle-leg switches, which can reduce the cost of the converter. While the ZVZCS T-type converter has more passive components than the ZVS T-type converter, the cost of these components is more than offset by the savings that result from the reduction of the current stresses in the middle switches. Since current in these switches is practically eliminated, devices that are much smaller and cheaper can be used. This is also true of the heatsinks for these switches as much less power is dissipated in them. As for the additional passive components in the ZVZCS T-type converter, these components conduct a small amount of current over a small fraction of the switching cycle so that inexpensive, low current-rated components can be used. Given the cost-savings related to the reduction of current-stresses in the middle switches and the low cost of the additional passive auxiliary circuit in the secondary, the ZVZCS T-type converter is actually less expensive than the regular ZVS T-type converter.

In order to compare the current stress in the converter switches for both the ZVS and ZVZCS T-Type converters, normalized rms and average currents for both converters with respect to the rms and average current of the main switches in ZVZCS converter for different transformer turns ratios (n) are shown in Fig. 5. It can be seen from Figs. 5(a), 5(b), 5(e), and 5(f) that the normalized currents of the main switches are almost same for both converters under heavy-load operating conditions, but, under light load operation, the rms current of main switches is higher because of the current hump that is caused by the charging of $C_{\mathrm{aux}}$ ($I_{peak}$ at (6)) and it is load-independent. It can be seen from Figs. 5(c), 5(d), 5(g), and 5(h) that the rms and average current of middle-leg switches of the ZVZCS converter are considerably smaller than those of the ZVS T-type converter.

## IV. COMPARISON OF POWER LOSSES IN SWITCHES

In this section, just the key power losses in the converter switches of the T-Type ZVS and ZVZCS converters are compared to simplify the discussion. The core losses are almost identical based on the discussion presented in [9], which compared the ZVS-PWM FB converter with a ZVS T-type converter. Any power losses due to the addition of the passive auxiliary circuit at the secondary were found to be insignificant and thus have been neglected. The comparison is focused on switch losses as these losses represent the most significant differences in the losses between the ZVS T-type and ZVZCS T-type converters. The two main sources of power losses in the primary side are switching losses and conduction losses. These power losses are compared for both the ZVS T-type and ZVZCS T-type converters as follows:

### A. SWITCHING LOSSES

Switching power losses are caused by the dissipation of stored energy in the parasitic capacitance of the switch [4] and can

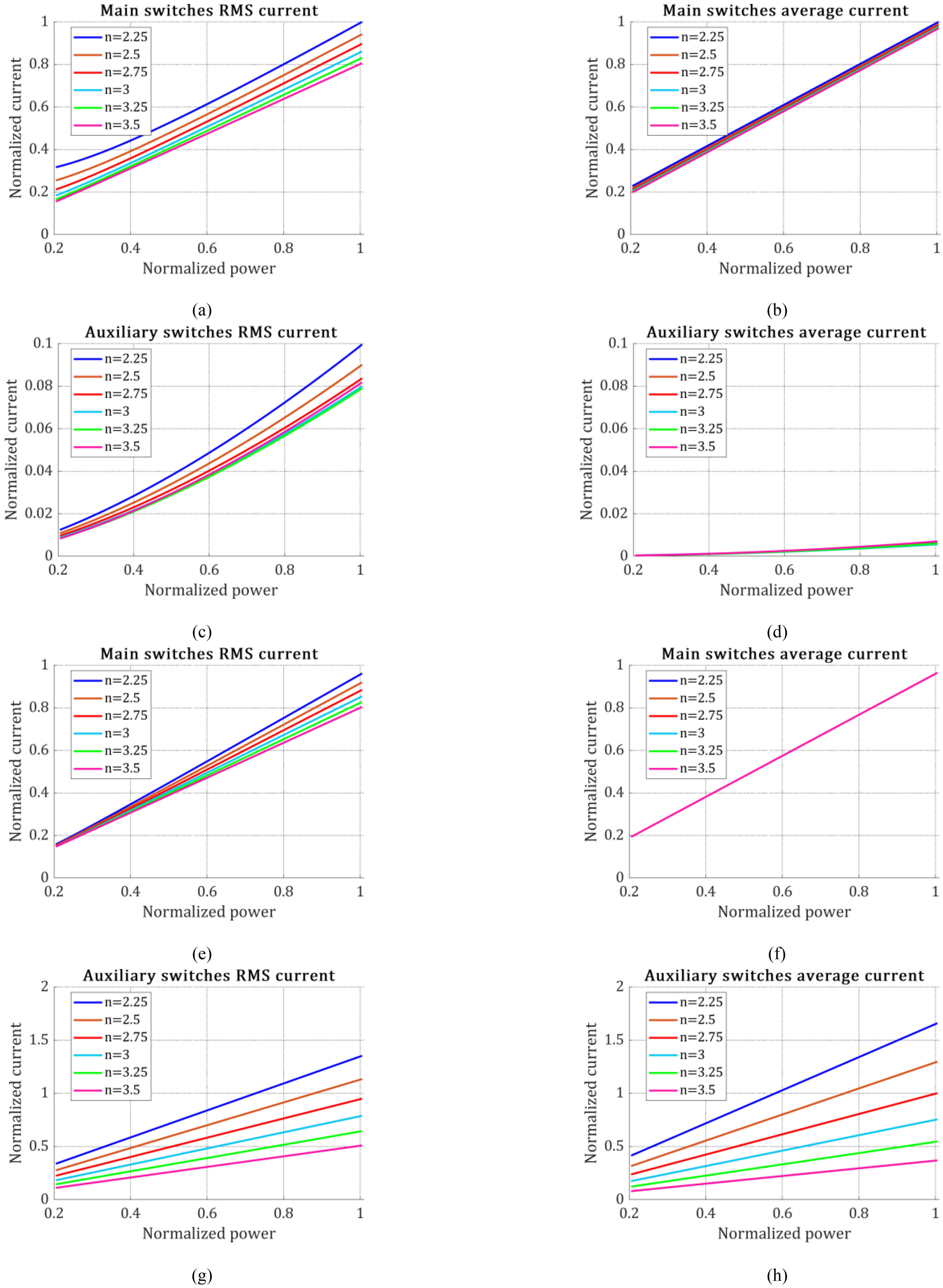


**FIG. 5.** Normalized current stress on converter switches for different transformer turns ratio (n), (a) Normalized ZVZCS T-type converter main switches rms current, (b) Normalized ZVZCS T-type converter main switches average current, (c) Normalized ZVZCS T-type converter auxiliary switches rms current, (d) Normalized ZVZCS T-type converter auxiliary switches average current, (e) Normalized ZVS T-type converter main switches rms current, (f) Normalized ZVS T-type converter main switches average current, (g) Normalized ZVS T-type converter auxiliary switches rms current, (h) Normalized ZVS T-type converter auxiliary switches average current.

be expressed as

$$P_{sw} = f_{sw}\left(\frac{1}{2}C_{oss}{V_s}^2\right) \tag{19}$$

where $f_{sw}$ is the switching frequency, $C_{oss}$ is the parasitic capacitance of the switch, and $V_s$ is the switch voltage when the switch is turned on.

In the ZVS T-Type converter, the voltage across the main switches (HV-switches) when they are about to be turned on can be expressed as

$$V_{S-HV}\left(t_{turn-on}\right) = \frac{V_{in}}{2} - Z_o I_3 \sin\left(\omega_0 t_{dt}\right) \tag{20}$$

where $t_{dt}$ is the dead time and $Z_o$ and $\omega_0$ are the characteristic impedance and resonance frequency of the resonant tank respectively and are defined as

$$Z_o = \sqrt{\frac{L_{lk}}{\frac{8}{3}C_{s-HV} + \frac{4}{3}C_{s-LV}}} \tag{21}$$

$$\omega_0 = \frac{1}{\sqrt{L_{lk}\left(2C_{S-HV} + C_{S-LV}\right)}} \tag{22}$$

where $C_{S-HV}$ and $C_{S-LV}$ are the parasitic capacitances of the main and middle-leg switches, respectively.

The turn-on power dissipation of the main switches of the ZVZCS converter is constant and independent of the load as the voltage across the switches is $V_{in}/2$ for all operating conditions. The power losses of a MOSFET during the turn-off process can be expressed as [27]

$$P_{sw-off} = \frac{1}{2}t_{off} I_{sw}\left(t_{\text{turn-off}}\right) V_{sw}\left(t_{\text{turn-off}}\right) \tag{23}$$

### B. CONDUCTION LOSSES

The power losses of the converter MOSFETs when they are on and the power losses of the transformer windings can be modeled as ohmic power losses. Moreover, the conduction losses in a MOSFET when current flows through its body diode can be expressed as the product of the diode voltage drop and the average value of the current. Taking these considerations into account, a mathematical expression for the conduction losses in a T-type converter can be derived as follows [25]:

$$\begin{aligned} P_{cond} = {} & \sqrt{2}\left(I_{et-rms}^2 \times R_{ds-HV} + I_{fw-rms}^2 \times R_{ds-LV}\right) \\ & + 0.5 I_{fw-ave} \times V_{Sdiode-LV} + \left(I_{fw-rms}^2 + I_{et-rms}^2\right) R_{pri}^2 \\ & + \left(I_{fw-rms}^2 + I_{et-rms}^2\right) n R_{sec}^2 \end{aligned} \tag{24}$$

where $R_{ds-HV}$, $R_{ds-LV}$ denote main and middle-leg switch on-state resistance respectively, $V_{Sdiode-LV}$ is the voltage drop across the body diode of the middle-leg switches, $I_{fw-ave}$is the average value of the freewheeling current, and $I_{et-rms}$, $I_{fw-rms}$, are the rms value of the energy transfer current, freewheeling current, respectively.

The current values for a ZVS T-type converter can be expressed as follows [25]:

$$I_{et-rms-ZVS} = \sqrt{D\left(I_2 I_1 + \frac{1}{3}(I_2 - I_1)^2\right)} \tag{25}$$

$$I_{fw-ave-ZVS} = \left(\frac{I_2 + I_3}{2}\right)(1 - D) \tag{26}$$

$$I_{fw-rms-ZVS} = \sqrt{1-D}\sqrt{I_3 I_2 + \frac{1}{3}(I_2 - I_3)^2} \tag{27}$$

### C. POWER LOSS BREAKDOWN

The power loss breakdown for both the ZVS and ZVZCS T-type converters can be calculated with the same method as in [28]. A comparison of loss analysis between the ZVS T-type and the conventional ZVS-PWM-FB converter was made in [17] and thus will not be presented here to limit paper size. The loss breakdown of the ZVS and ZVZCS T-type converters when they are operating with 30% of rated load and with full rated load are shown in Fig. 6. It can be seen the power losses consist of two components: the power losses that are fixed regardless of using a ZVS or a ZVZCS topology and power losses that are dependent on the converter topology. Fig. 6(a) shows the power loss breakdown for the converters at 30% of the rated load. It can be seen that the conduction losses are higher in the ZVS T-type converter due to circulating current in freewheeling modes. For this load (30% of rated load), however, the circulating current is not enough to fully discharge the parasitic capacitors of the main switches ($S_1$ and $S_2$), and they are operated with partial ZVS so that the switching losses are not zero.

In the ZVZCS converter, conduction losses are smaller than the ZVS converter, but the switching losses are higher because the voltage across the switches are equal to $V_{in}/2$ at turn-on time. Fig. 6(a) shows the power loss breakdown for the converters at the rated load. It can be seen that switching losses of the ZVS converter are zero because the circulating current magnitude is enough to achieve ZVS at main switches, but the conduction losses are considerable. In the ZVZCS converter, switches, the conduction losses are reduced, but the main switches operate without ZVS. Since the voltage across the main switches is half of the input voltage, however, this results in an inherent 75% reduction of ½ $CV^2$ switching losses compared to the hard-switching operation of a switch in the ZVS-PWM-FB converter.

### D. ZVZCS VS. ZVS OPERATION

In summary, the middle-leg switches of the ZVS and ZVZCS T-type converters are always operated with ZVS because half the input voltage appears at their drain and at their source before they are turned on. For the main switches, under light-load condition for both the ZVZCS and ZVS converter, the switches are operated without ZVS because there is not enough inductive energy available for to discharge the output capacitances of the switches to ensure ZVS operation. The conduction losses that exist during the freewheeling mode and that reduce the converter efficiency of the ZVS converter are, however, reduced in the ZVZCS converter because the freewheeling current is extinguished.

As the converter load is increased, the switches in the ZVS converter can operate with ZVS, but the conduction losses in the primary side during the freewheeling mode offsets the power loss savings from ZVS operation so that both the ZVZCS and ZVS converter has almost the same efficiency.

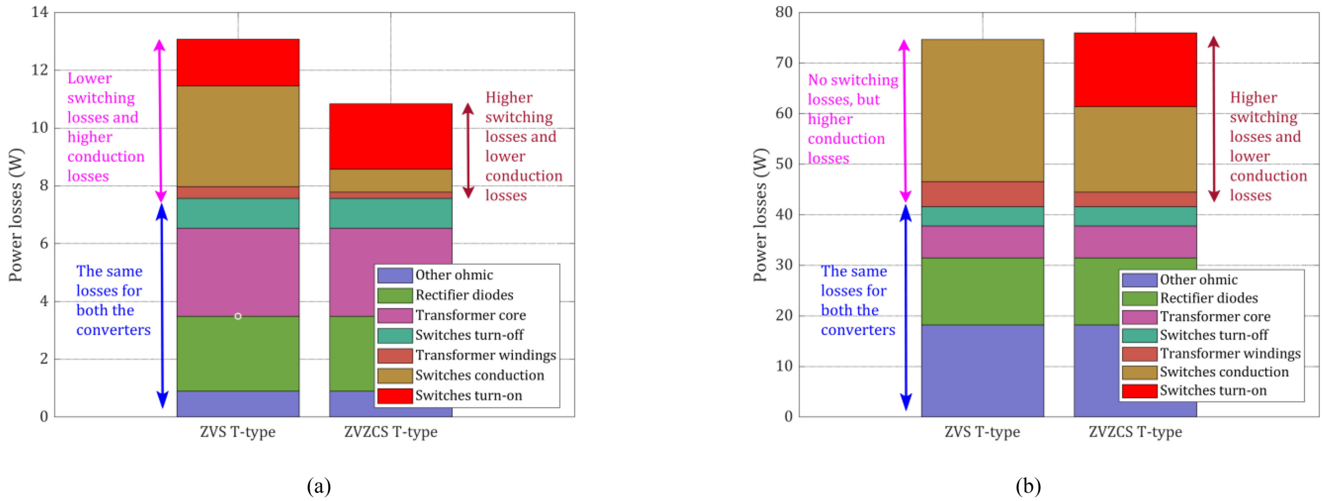


**FIG. 6.** **Loss breakdown for the T-type and ZVS-PWM-FB converters. (a) 30% load, (b) rated load.**

**TABLE I** **Specification of the Converter Components**

| Symbol | Item | Value |
|---|---|---|
| $V_{in}$ | Input voltage | 400V |
| $V_o$ | Output voltage | 48V |
| $P_{o,max}$ | Maximum output power | 900W |
| $P_{o,min}$ | Minimum output power | 45W |
| $f_{sw}$ | Switching frequency | 50 kHz |
| $S_1, S_2$ | Main switches for both the converters | FDP18N50 |
| $S_3, S_4$ | Middle leg switches for ZVS T-Type converter | FDP51N25 |
| $S_3, S_4$ | Middle leg switches for ZVZCS T-Type converter | FQP3N30 |
| $R_{DS(on)\text{-}S1,\,S2}$ | Main switches turn on resistance | 220 mΩ |
| $R_{DS(on)\text{-}S3,\,S4}$ | Middle leg switches turn on resistance for ZVS T-Type converter | 60 mΩ |
| $R_{DS(on)\text{-}S3,\,S4}$ | Middle leg switches turn on resistance for ZVZCS T-Type converter | 2.2Ω |
| n | The turns ratio of the transformer | 2.5:1:1 |

As the converter load is further increased there will be a point where the difference in the efficiency of the two converters becomes noticeable.

## VI. EXPERIMENTAL RESULTS

Prototypes of the ZVS T-Type converter and ZVZCS T-Type converter were built according to the specifications in Table I. For both converters, the same MOSFET devices were used for $S_1$ and $S_2$. For the ZVS T-Type converter, MOSFETs with low voltage ratings and low $R_{ds\text{-}on}$ were used as $S_3$ and $S_4$. For the ZVZCS T-Type converter, MOSFETs with low voltage rating and high $R_{ds\text{-}on}$ were used as $S_3$ and $S_4$. It should be noted that the $R_{ds\text{-}on}$ of the middle-leg switches of the ZVZCS converter is more than 36 times higher than that of the $R_{ds\text{-}on}$ of the middle- leg switches of the ZVS converter. Devices with a much higher $R_{ds\text{-}on}$ value were chosen on purpose as such devices are less expensive and have lower $C_{oss}$ values. The retail price of the middle leg switches in ZVZCS converter is almost 40% of the middle leg switches in the ZVS converter at the time of this writing [15], [16].

Typical waveforms of ZVZCS and ZVS T-type converters are shown in Fig. 7 and Fig. 8, respectively. Fig 7(a) shows the voltage across one of the main switch ($V_{S1}$), an auxiliary switch ($V_{S3}$), transformer primary current ($I_{pri}$), and the gate-source voltage of $S_1$ ($V_{g1}$). This figure shows that $S_1$ is turned-on with half of the input voltage and the auxiliary switch is turned on with ZVS. The primary current waveform shows that the current is extinguished by the auxiliary circuit during freewheeling modes.

Fig. 7(b) shows $V_{S1}$, $I_{pri}$, $V_{g1}$, and $V_{g4}$ at 30% of the rated load. It can be seen from this figure that circulating current is zero, and $V_{S1}$ remains at $V_{in}/2$ at turn-on time. Fig. 7(c) shows the same waveforms as Fig. 7(b) at 100% of rated load. It can be seen that even under heavy-load operation condition, $I_{pri}$ vanishes, and $V_{S1}$ remains at $V_{in}/2$ at turn-on time.

Fig. 8 shows the same waveforms as Fig. 7 for the ZVS T-type converter. It can be seen from Fig 8(a) that, like the ZVZCS converter, the auxiliary switches turn-on with ZVS. The ZVS operation of main switches depends on the available energy to discharge the parasitic capacitor of the switches. As can be seen from Fig 8(b) when the ZVS converter is operated under light load, the circulating current does not vanish during freewheeling modes; however, due to a lack of inductive energy, the main switches are operated with partial ZVS so that neither conduction losses nor switching losses are zero. As can be seen from Fig 8(c), when the load increases, the available inductive energy for ZVS operation increases and the main switches are operated with ZVS. The cost of ZVS operation, however, is higher current ratings for the auxiliary switches and conduction losses that offset power saving due to ZVS operation in T-type converters.

For the sake of comparison, prototypes of the ZVS-PWM-FB converter and ZVZCS-PWM-FB converter were also built according to the same specifications as in [25]. A graph of

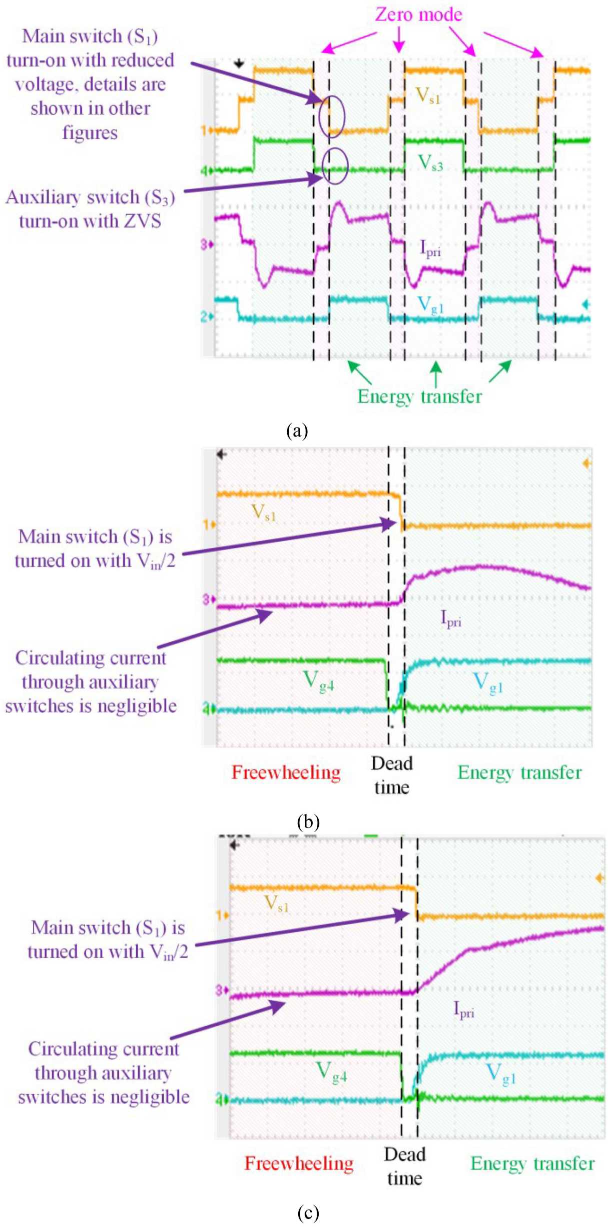


**FIG. 7.** **Typical converter waveforms of a ZVZCS T-type converter. (a) Voltage across switches S1 and S3, the current waveform of the transformer primary, gate-source voltage of S1(V: 250V/div, I: 5A/div., Vgs: 10V/div, t: 5 μs/div.), (b) Voltage across switches S1, the current waveform of the transformer primary, gate-source voltage of S1 and S4 at 30% of rated load (V: 250V/div, I: 1A/div., Vgs: 10V/div, t: 250 ns/div.), (c) Voltage across switches S1, the current waveform of the transformer primary, gate-source voltage of S1 and S4 at 100% of rated load (V: 250V/div, I: 5A/div., Vgs: 10V/div, t: 250 ns/div.).**

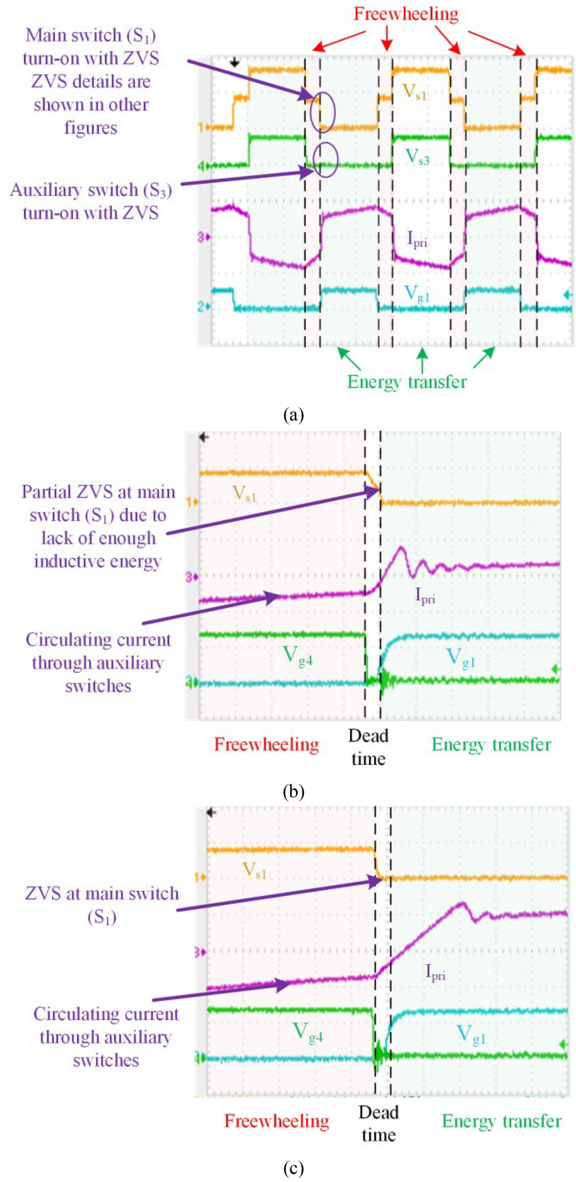


**FIG. 8.** **Typical converter waveforms of a ZVS T-type converter. (a) Voltage across switches S1 and S3, the current waveform of the transformer primary, gate-source voltage of S1(V: 250V/div, I: 5A/div., Vgs: 10V/div, t: 5 μs/div.), (b) Voltage across switches S1, the current waveform of the transformer primary, gate-source voltage of S1 and S4 at 30% of rated load (V: 250V/div, I: 1A/div., Vgs: 10V/div, t: 250 ns/div.), (c) Voltage across switches S1, the current waveform of the transformer primary, gate-source voltage of S1 and S4 at 100% of rated load (V: 250V/div, I: 5A/div., Vgs: 10V/div, t: 250 ns/div.).**

efficiency vs. load curves for all four prototypes are shown in Fig. 9. The following should be noted:

- The two T-type converters are more efficient than the ZVS-PWM-FB and ZVZCS-PWM-FB converters for light loads, but less efficient than these converters for heavy loads. This is due to the fact that the T-type converters are based on half-bridge converters, as explained in Section I and to the fact that the middle-leg switches can always operate with ZVS even under light-load conditions, as explained in Section II.
- Using ZVZCS improves light-load efficiency for both the T-Type converter and the PWM-FB converter, at the cost of worsening heavy-load efficiency. This is because the ZVZCS converters do not operate with full ZVS at heavy loads while the other two converters do; thus, they have turn-on switching losses that the other converters

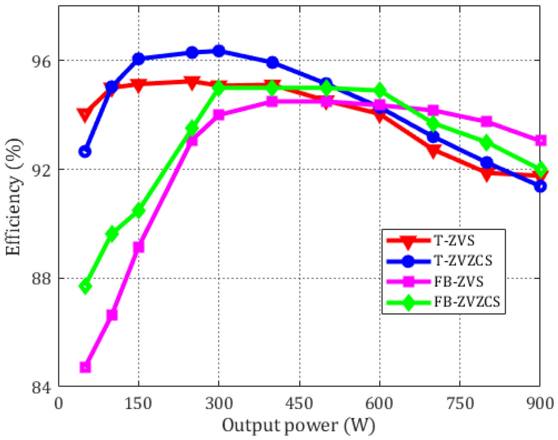


**FIG. 9.** **Graph of efficiency vs output power for the ZVS T-Type and ZVZCS T-Type converters.**

do not. Under light-load conditions, switching losses exist in all the converters, but the ZVZCS eliminates all freewheeling current losses and turn-off losses.

- The most efficient converter for heavy-loads is the ZVS-PWM-FB converter. The most efficient converter for light-load operation is the ZVZCS T-Type converter.
- When comparing the two T-type converters vs the ZVS-PWM-FB converter, which is the most efficient heavy-load converter, the crossover point in load when the ZVS-PWM-FB converter becomes more efficient than a T-type converter occurs at a higher load for the ZVZCS T-type converter than for the ZVS T-type converter, by about 100 W. This allows the T-Type converter to operate with higher efficiency than the ZVS-PWM-FB converter over a wider load range.
- It is only at extremely light-loads (5% of rated load) that the ZVS T-type converter is more efficient than the ZVZCS T-Type converter. This is because there is a very little current flowing in the converter so that any losses that are saved due to the passive secondary-side auxiliary circuit are more than offset by the passive auxiliary circuit losses, which are few. It is only when there is some current flowing in the primary that the current-related losses saved by the auxiliary circuit offset the losses it generates. These very light loads are considered to be outside the range of typical operation (> 10 % load). From a practical point-of-view, this translates into a loss difference of less than 1 W.
- Throughout the load range, the ZVZCS T-type converter has better or almost the same efficiency as the ZVS T-Type converter, but its middle-leg switches have negligible current stress and can be implemented with less expensive devices.

## VII. CONCLUSION

Light-load converter efficiency has become more important in recent years due to the widespread use of power electronics in society. In many applications, power converters operate at full-load occasionally and mostly operate under lighter load conditions. In their previous work, the authors proposed the use of the ZVS T-type converter as a way to improve light-load efficiency. The use of ZVZCS methods in T-Type converters is proposed in this paper to minimize the freewheeling mode circulating current in the primary, which further improves light-load efficiency and reduces the amount of RMS current that the middle-leg switches of the converter.

In this paper, the operation of the ZVS T-Type converter and a T-Type converter with ZVZCS are explained and analyzed. Results obtained from experimental prototypes of the two converters are presented along with experimental results of obtained from prototypes of the standard ZVS-PWM full-bridge converter and a ZVZCS-PWM full-bridge converter.

The main contributions of this work to the power electronics literature are as follows:

- With the exceptions of very light loads that are outside the range of normal operation, the ZVZCS T-Type converter is the most efficient converter for light-load operation among the four options. For an application that requires an inexpensive silicon-based MOSFET converter to operate typically with ≤ 500 W (with only occasional heavy-load operation), the ZVZVS T-type converter is a very attractive option.
- The middle-leg switches of the T-type converter must block only half the input DC voltage and must conduct a very small amount of current, especially compared to the standard ZVS-PWM-FB converter. This allows cheaper, less expensive devices to the used as the middle-leg switches as the current through these devices is practically negligible, unlike that of any of the switches in a ZVS-PWM-FB converter or the middle-leg switches or a ZVS T-type converter. It also shrinks the size of the devices themselves and opens the door to implementing these middle-leg devices in an integrated circuit (IC), thus reducing the size of the overall converter significantly.
- The work presented in this paper is an advance over the authors' previous work that was presented in [25], in terms of light-load converter efficiency and middle-leg switch RMS current stress.

To the best of the authors' knowledge, these contributions have not been presented in the literature. It should be noted that any control method that can be used in a ZVS-PWM FB converter to improve light-load efficiency can be used to the ZVZCS T-type converter. There is nothing that prevents this from being done, given both converters are able to impress an AC square-wave across the primary of their transformer.

## REFERENCES

[1] R. Redl, N. O. Sokal, and L. Balogh, "A novel soft-switching full-bridge DC/DC converter: Analysis, design considerations, and experimental results at 1.5 kW, 100 kHz," *IEEE Trans. Power Electron.*, vol. 6, no. 3, pp. 408–418, Jul. 1991.

[2] Y. Jang and M. M. Jovanović, "A new PWM ZVS full-bridge converter," *IEEE Trans. Power Electron.*, vol. 22, no. 3, pp. 987–994, May 2007.

[3] M. K. Yang, H. S. Cho, S. J. Lee, and W. Y. Choi, “High-efficiency soft-switching PWM DC-DC converter for electric vehicle battery chargers,” in *Proc. IEEE Energy Convers. Congr. Expo.*, 2013, pp. 1092–1095.
[4] M. Kasper, R. M. Burkart, G. Deboy, and J. W. Kolar, “ZVS of power MOSFETs revisited,” *IEEE Trans. Power Electron.*, vol. 31, no. 12, pp. 8063–8067, Dec. 2016.
[5] A. Vazquez, A. Rodriguez, D. G. Lamar, and M. M. Hernando, “Advanced control techniques to improve the efficiency of IPOP modular QSW-ZVS converters,” *IEEE Trans. Power Electron.*, vol. 33, no. 1, pp. 73–86, Jan. 2018.
[6] D. Christen and J. Biela, “Analytical switching loss modeling mased on datasheet parameters for MOSFETs in a half-bridge,” *IEEE Trans. Power Electron.*, vol. 34, no. 4, pp. 3700–3710, Apr. 2019.
[7] A. Safaee, P. K. Jain, and A. Bakhshai, “An adaptive ZVS full-bridge DC-DC converter with reduced conduction losses and frequency variation range,” *IEEE Trans. Power Electron.*, vol. 30, no. 8, pp. 4107–4118, Aug. 2015.
[8] A. Safaee, P. Jain, and A. Bakhshai, “A ZVS pulsewidth modulation full-bridge converter with a low-RMS-current resonant auxiliary circuit,” *IEEE Trans. Power Electron.*, vol. 31, no. 6, pp. 4031–4047, Jun. 2016.
[9] L. Zhao, H. Li, X. Wu, and J. Zhang, “An improved phase-shifted full-bridge converter with wide-range ZVS and reduced filter requirement,” *IEEE Trans. Ind. Electron.*, vol. 65, no. 3, pp. 2167–2176, Mar. 2018.
[10] L. Zhao, H. Li, C. Xu, and X. Zheng, “Efficiency improvement of an adaptive-energy-storage full-bridge converter by modifying turns ratio of a coupled inductor,” *IEEE Trans. Power Electron.*, vol. 33, no. 2, pp. 948–956, Feb. 2018.
[11] G. Ortiz, L. Fassler, J. W. Kolar, and O. Apeldoorn, “Flux balancing of isolation transformers and application of ‘The magnetic ear’ for closed-loop volt-second compensation,” *IEEE Trans. Power Electron.*, vol. 29, no. 8, pp. 4078–4090, Aug. 2014.
[12] M. Pahlevaninezhad, S. Eren, P. K. Jain, and A. Bakhshai, “Self-sustained oscillating control technique for current-driven full-bridge DC/DC converter,” *IEEE Trans. Power Electron.*, vol. 28, no. 11, pp. 5293–5310, Nov. 2013.
[13] S. M. Kaviri, H. Hajebrahimi, S. Eren, and M. Pahlevani, “A digital active DC-eliminating method for DC/DC converters,” *IEEE Trans. Power Electron.*, vol. 34, no. 4, pp. 3014–3019, Apr. 2019.
[14] S. H. Kim, H. Cha, H. F. Ahmed, B. Choi, and H. G. Kim, “Isolated double step-down dc-dc converter with improved ZVS range and no transformer saturation problem,” *IEEE Trans. Power Electron.*, vol. 32, no. 3, pp. 1792–1804, Mar. 2017.
[15] H. F. Ahmed, H. Cha, A. A. Khan, and H. G. Kim, “A family of high-frequency isolated single-phase Z-source AC-AC converters with safe-commutation strategy,” *IEEE Trans. Power Electron.*, vol. 31, no. 11, pp. 7522–7533, Nov. 2016.
[16] D. G. Bandeira, S. A. Mussa, and I. Barbi, “A ZVS-PWM T-type isolated DC-DC converter,” in *Proc. IEEE 13th Brazilian Power Electron. Conf. 1st Southern Power Electron. Conf.*, 2015, pp. 1–6.
[17] J. Khodabakhsh and G. Moschopoulos, “A study of T-type and ZVS-PWM full-bridge converters for switch-mode power supplies,” *IEEE Trans. Power Electron.*, vol. 35, no. 7, pp. 7145–7159, Jul. 2020.
[18] ENERGY STAR, “ENERGY STAR Program Requirements for Computers Partner Commitments,” 2014.
[19] J. K. Han and G. W. Moon, “High-efficiency phase-shifted full-bridge converter with a new coupled inductor rectifier (CIR),” *IEEE Trans. Power Electron.*, vol. 34, no. 9, pp. 8468–8480, Sep. 2019.
[20] L. C. Shih, Y. H. Liu, and H. J. Chiu, “A novel hybrid mode control for a phase-shift full-bridge converter featuring high efficiency over a full-load range,” *IEEE Trans. Power Electron.*, vol. 34, no. 3, pp. 2794–2804, Mar. 2019.
[21] T. T. Song, N. Huang, and A. Ioinovici, “A zero-voltage and zero-current switching three-level DC-DC converter with reduced rectifier voltage stress and soft-switching-oriented optimized design,” *IEEE Trans. Power Electron.*, vol. 21, no. 5, pp. 1204–1212, Sep. 2006.
[22] M. Pahlevaninezhad, P. Das, J. Drobnik, P. K. Jain, and A. Bakhshai, “A novel ZVZCS full-bridge DC/DC converter used for electric vehicles,” *IEEE Trans. Power Electron.*, vol. 27, no. 6, pp. 2752–2769, Jun. 2012.
[23] J. G. Cho, J. A. Sabaté, G. Hua, and F. C. Lee, “Zero-voltage and zero-current-switching full bridge PWM converter for high-power applications,” *IEEE Trans. Power Electron.*, vol. 11, no. 4, pp. 622–628, Jul. 1996.
[24] J. G. Cho, J. W. Back, C. Y. Jeong, and G. H. Rim, “Novel zero-voltage and zero-current-switching full-bridge PWM converter using a simple auxiliary circuit,” *IEEE Trans. Ind. Appl.*, vol. 35, no. 1, pp. 15–20, Jan. 1999.
[25] J. Khodabakhsh and G. Moschopoulos, “A study of T-type and ZVS-PWM full-bridge converters for switch-mode power supplies,” *IEEE Trans. Power Electron.*, vol. 35, no. 7, pp. 7145–7159, Jul. 2020.
[26] B.-H. Choo, B. Lee, S.-B. Yoo, and D.-S. Hyun, “A novel secondary clamping circuit topology for soft switching full-bridge PWM DC/DC converter,” in *Proc. IEEE, APEC ’98 13th Ann. Appl. Power Electron. Conf. Expo.*, 1998, vol. 2, pp. 840–845.
[27] R. W. Erickson and D. Maksimović, in *Fundamentals of Power Electronics*. Boston, MA, USA: Springer US, 2001.
[28] B. Y. Chen and Y. S. Lai, “Switching control technique of phase-shift-controlled full-bridge converter to improve efficiency under light-load and standby conditions without additional auxiliary components,” *IEEE Trans. Power Electron.*, vol. 25, no. 4, pp. 1001–1012, Apr. 2010.
[29] “FQP3N30 ON Semiconductor | Discrete Semiconductor Products | DigiKey,” Nov. 2013. [Online]. Available: https://www.digikey.ca/product-detail/en/on-semiconductor/FQP3N30/FQP3N30-ND/1053944 Accessed: Jul. 7, 2019
[30] “FDP51N25 ON Semiconductor | Discrete Semiconductor Products | DigiKey,” Mar. 2016. [Online]. Available: https://www.digikey.ca/product-detail/en/on-semiconductor/FDP51N25/FDP51N25-ND/1922994 Accessed: Jul. 7, 2019

**JAVAD KHODABAKHSH** (Student Member, IEEE) received the M.Sc. degree in electrical engineering from the University of Tehran, Tehran, Iran, in 2006, and the Ph.D. degree in electrical engineering from Western University, London, ON, Canada, in 2019. He is a Researcher at Western University. From 2007 to 2015, he was a tenured Lecturer with the Azad University, Tehran, Iran, and working as an Electrical Design Engineer in various industrial projects (oil & gas, mine & metal), Tehran, Iran. His research interests include power electronic converters for utility applications, microgrid operation, and renewable energy systems. He is a member of the Ontario Society of Professional Engineers (OSPE).

**GERRY MOSCHOPOULOS** (Senior Member, IEEE) received the B.Eng., M.A.Sc., and Ph.D. degrees from Concordia University, Montreal, QC, Canada, in 1989, 1992, and 1997, respectively, all in electrical engineering. From 1996 to 1998, he was a Design Engineer in the Advanced Power Systems Division, Nortel Networks, Lachine, QC, Canada. From 1998 to 2000, he was a Postdoctoral Fellow at Concordia University, where he was involved in research in the area of power electronics for telecommunications applications. He joined the Department of Electrical and Computer Engineering at Western University, London, ON, Canada in 2000 and is currently a Professor there.

He has authored or co-authored more than 200 technical papers and one book. He was Co-Technical Chair of the IEEE International Communications Energy Conference (INTELEC) in 2014, Co-Technical Chair of the IEEE Canadian Conference on Electrical and Computer Engineering (CCECE) in 2012 and 2014, and the Technical Chair of the IEEE Electrical Power and Energy Conference (EPEC) in 2015. He is currently an Associate Editor for the IEEE Transactions on Power Electronics and the IEEE Journal of Emerging and Selected Topics in Power Electronics. He is a Registered Professional Engineer in the province of Ontario.